

**CATALYTIC CO-PYROLYSIS OF SUGARCANE
BAGASSE AND WASTE PLASTICS USING
ZEOLITE AND HYDROXYAPATITE BASED
CATALYST FOR HIGH QUALITY PYROLYSIS
OIL IN A FIXED-BED REACTOR**

HAMIZURA BT HASSAN

UNIVERSITI SAINS MALAYSIA

2019

**CATALYTIC CO-PYROLYSIS OF SUGARCANE
BAGASSE AND WASTE PLASTICS USING
ZEOLITE AND HYDROXYAPATITE BASED
CATALYST FOR HIGH QUALITY OF
PYROLYSIS OIL IN A FIXED-BED REACTOR**

by

HAMIZURA BT HASSAN

**Thesis submitted in fulfilment of the
requirements for the degree of
Doctor of Philosophy**

July 2019

ACKNOWLEDGEMENT

First and foremost, I would like to express my sincere gratitude and acknowledgement to my supervisor, Professor Dr. Bassim H. Hameed for his patience, guidance, immense knowledge and motivation throughout my Ph.D study. His dedication and enthusiasm in research really inspired and motivated me, especially during the tough time in my Ph.D pursuit. A special thanks to Prof. Dr. Lim Jit Kang, my co-supervisor, for his insightful comments and encouragement during this research. Furthermore, I would like to thank all the technical and administrative staff at the School of Chemical Engineering, for their valuable help and cooperation. I would like to acknowledge the Ministry of Higher Education (MOHE), Malaysia and the Universiti Teknologi MARA (UiTM) for the scholarship support. I also sincerely thank the research grants provided by the Universiti Sains Malaysia, Malaysia under Research University (RU) TOP-DOWN grant for funding these works. Special thanks to the members of READ especially Dr. Yee Ling Tan, Dr. Kabir Garba, Dr Norhaslinda Nasuha, Norhayati and Mutmirah, for their helping hand and kind support.

I would like to express my heartfelt love and gratitude to my parents; Hassan Jasin and Norrishah Yaakub and my sisters Hasmilizawati and Hazila for their unconditional love and emotional support. I am forever indebted to my husband, Musa Mohamed Zahidi for his unconditional love, assistance and endless encouragement. The last word goes to my baby boy, Lukman Harith, who has given me an extra strength and motivation to complete this Ph.D journey.

Hamizura Hassan

July 2019

TABLE OF CONTENTS

	Page
ACKNOWLEDGEMENT	ii
TABLE OF CONTENTS	iii
LIST OF TABLES	ix
LIST OF FIGURES	xi
LIST OF PLATES	xvii
LIST OF SYMBOLS	xviii
LIST OF ABBREVIATIONS	xix
ABSTRAK	xxii
ABSTRACT	xxiv
CHAPTER 1 INTRODUCTION	1
1.1 Global Demand for Alternative Energy Sources	1
1.2 Biomass-Derived Bio-Oil	2
1.3 Catalytic Pyrolysis of Biomass	3
1.4 Catalytic Co-Pyrolysis	4
1.5 Problem Statement	7
1.6 Objectives of the Study	9
1.7 Scope of Study	10
1.8 Thesis Organization	11
CHAPTER 2 LITERATURE REVIEW	13
2.1 Introduction	13
2.2 Feedstock for Co-Pyrolysis Process	13
2.2.1 Lignocellulosic Biomass	13
2.2.1(a) Components of Lignocellulosic Biomass	15
2.2.2 Synthetic Polymers	17
2.3 Co-Pyrolysis Process	20
2.4 Effect of Operating Conditions on Co-Pyrolysis of Biomass and Plastic	28
2.4.1 Effect of Reaction Temperature on Product Yield and Chemical Composition of Bio-Oil	28
2.4.2 Effect of Biomass-To-Plastic Ratio on Product Yield and Chemical Composition of Bio-Oil	30

2.5	Catalytic Co-Pyrolysis of Biomass and Plastics	31
2.5.1	Reaction Mechanism of Biomass-Plastics Catalytic Co-Pyrolysis	33
2.5.2	Function of Catalyst in Co-Pyrolysis of Biomass	36
2.5.2(a)	Microporous Catalyst	37
2.5.2(b)	Mesoporous catalyst	39
2.5.3	Effect of Operating Conditions on Catalytic Co-Pyrolysis of Biomass and Plastic	42
2.5.3(a)	Effect of Reaction Temperature on Product Yields and Chemical Composition of Bio-Oil	42
2.5.3(b)	Effect of Catalyst Loading on Product Yields and Chemical Composition of Bio-Oil	44
2.5.3(c)	Effect of Biomass-To-Plastic Blending Ratio on Product Yields and Chemical Composition of Bio-Oil	46
2.6	Chemical Composition of Bio-Oil Obtained from Catalytic Co-Pyrolysis	47
2.7	Product Fractional Yield Obtained from Catalytic Co-Pyrolysis of Biomass and Plastic	51
2.8	Kinetic of Thermal, Co-Pyrolysis and Catalytic Co-Pyrolysis of Biomass and Plastic by Thermogravimetric	54
2.9	Summary	61
	CHAPTER 3 METHODOLOGY	62
3.1	Introduction	62
3.2	Experimental Flow	62
3.3	Materials and Chemicals	65
3.3.1	Materials	65
3.3.2	Chemicals	65
3.4	Description of Fixed-Bed Reactor Set-Up	66
3.5	Biomass, Plastic and Product Characterization	69
3.5.1	Proximate Analysis	69
3.5.2	Elemental Analysis	70
3.5.3	Gas Chromatography-Mass Spectrometry (GCMS)	70
3.5.4	Gas Chromatography with Thermal Conductivity Detector (GC-TCD)	71
3.5.5	High Heating Value	71

3.6	Catalyst Characterization	71
3.6.1	Nitrogen Adsorption-Desorption	72
3.6.2	X-ray Fluorescence (XRF)	72
3.6.3	X-ray Diffraction (XRD)	73
3.6.4	Scanning Electron Microscopy with Energy Dispersive X-ray (SEM-EDX)	73
3.6.5	Ammonia-Temperature-Programmed Desorption (NH ₃ -TPD)	73
3.7	Synthesis of Catalysts	74
3.7.1	Synthesis of Faujasite-electric Arc Furnace Slag Zeolite (FAU-EAFS) Catalyst	74
3.7.2	Synthesis of Hydroxyapatite-Zeolite (HAP-ZE) Composite Catalyst	75
3.8	Pyrolysis Reaction	75
3.8.1	Thermal Co-pyrolysis	76
3.8.2	Catalytic Co-pyrolysis	77
3.9	Synergistic Effect	78
3.9.1	Synergistic Effect During Co-pyrolysis	78
3.9.2	Synergistic Effect During Catalytic Co-pyrolysis	79
3.10	Kinetic Study	79
	CHAPTER 4 RESULTS AND DISCUSSION	83
4.1	Introduction	83
4.2	Characterization of Feedstock	84
4.2.1	Proximate and Ultimate Analysis of Feedstock	84
4.2.2	Thermal Degradation Characteristic of Feedstocks	86
4.3	Thermal Pyrolysis of Feedstock	88
4.4	Co-pyrolysis of Sugarcane Bagasse with High-Density Polyethylene and Polyethylene Terephthalate	90
4.4.1	Effect of Reaction Temperature	90
4.4.1(a)	Co-pyrolysis Product Yield at Different Reaction Temperatures	90
4.4.1(b)	Chemical Composition of Pyrolysis Oil at Different Reaction Temperatures	96
4.4.1(c)	Gas compositions at different reaction temperatures	103
4.4.2	Effect of biomass-to-plastic ratio	106

4.4.2(a)	Co-pyrolysis product yield at different biomass-to-plastic ratio	106
4.4.2(b)	Chemical composition of pyrolysis oil at different biomass-to-plastic ratio	110
4.4.3	Elemental analysis and heating value of pyrolysis oil	118
4.4.4	Comparison of different plastic on product distribution and chemical composition in co-pyrolysis of sugarcane bagasse and plastics	120
4.5	Catalytic co-pyrolysis of sugarcane bagasse with high-density polyethylene and polyethylene terephthalate over Faujasite-electric arc furnace slag zeolite and Hydroxyapatite-zeolite catalysts	122
4.5.1	Characterization of Faujasite-electric arc furnace slag and Hydroxyapatite-Zeolite catalysts	122
4.5.1(a)	X-ray diffraction analysis (XRD) analysis	122
4.5.1(b)	Nitrogen adsorption-desorption	124
4.5.1(c)	Scanning electron microscopy –energy dispersive X-ray (SEM-EDX)	127
4.5.1(d)	NH ₃ temperature programmed desorption (NH ₃ -TPD)	130
4.6	Catalytic co-pyrolysis of sugarcane bagasse and high density polyethylene over Faujasite-electric arc furnace slag zeolite and hydroxyapatite-zeolite catalysts	132
4.6.1	Effect of reaction temperature	132
4.6.1(a)	Effect of reaction temperature on product fractional yield	132
4.6.1(b)	Effect of reaction temperature on chemical composition of pyrolysis oil	134
4.6.1(c)	Effect of reaction temperature on gas compositions	139
4.6.2	Effect of catalyst-to-feedstock ratio	141
4.6.2(a)	Effect of catalyst-to-feedstock ratio on product fractional yield	141
4.6.2(b)	Effect of catalyst-to-feedstock ratio on chemical composition of pyrolysis oil	143
4.6.3	Effect of SCB-to-HDPE blending ratio	146
4.6.3(a)	Effect of SCB-to-HDPE blending ratio on product fractional yield	147

4.6.3(b)	Effect of SCB-to-HDPE blending ratio on chemical compositions	148
4.6.4	Comparison between Faujasite-electric arc furnace slag zeolite and Hydroxyapatite-zeolite performances in catalytic co-pyrolysis of sugarcane bagasse with high-density polyethylene	154
4.6.5	Elemental analysis and heating values of pyrolysis oil obtained from co-pyrolysis of sugarcane bagasse and high density polyethylene over Faujasite-electric arc furnace slag zeolite and Hydroxyapatite-zeolite catalysts	156
4.7	Catalytic co-pyrolysis of sugarcane bagasse and polyethylene terephthalate over Faujasite-electric arc furnace slag zeolite and Hydroxyapatite-zeolite catalysts	157
4.7.1	Effect of reaction temperature	157
4.7.1(a)	Effect of reaction temperature on product fractional yield	157
4.7.1(b)	Effect of reaction temperature on chemical compositions of pyrolysis oil	159
4.7.1(c)	Effect of reaction temperature on gas compositions	164
4.7.2	Effect of catalyst-to-feedstock ratio	167
4.7.2(a)	Effect of catalyst-to-feedstock ratio on product fractional yield	167
4.7.2(b)	Effect of catalyst-to-feedstock ratio on chemical compositions of pyrolysis oil	169
4.7.3	Effect of SCB-to-PET ratio	173
4.7.3(a)	Effect of SCB-to-PET ratio on product fractional yield	173
4.7.3(b)	Effect of SCB-to-PET ratio on chemical compositions of pyrolysis oil	175
4.7.4	Comparison of product distributions in catalytic co-pyrolysis of sugarcane bagasse and polyethylene terephthalate over Faujasite-electric arc furnace slag zeolite and Hydroxyapatite-zeolite catalysts	181
4.7.5	Elemental analysis and heating values of pyrolysis oil obtained from co-pyrolysis of sugarcane bagasse and polyethylene terephthalate over Faujasite-electric arc furnace slag zeolite and Hydroxyapatite-zeolite catalysts	182

4.7.6	Comparison of types of plastic on product distributions and chemical compositions in catalytic co-pyrolysis of sugarcane bagasse and plastic	183
4.7.7	Comparison between co-pyrolysis and catalytic co-pyrolysis of sugarcane bagasse with plastics over Faujasite-electric arc furnace slag zeolite and Hydroxyapatite-zeolite catalysts	185
4.8	Thermal behaviour and kinetic study of catalytic co-pyrolysis of sugarcane bagasse and high-density polyethylene	188
4.8.1	Thermal, co-pyrolysis and catalytic co-pyrolysis behaviour of sugarcane bagasse and high-density polyethylene by using thermogravimetric analysis	188
4.8.2	Kinetic of thermal, co-pyrolysis and catalytic of co-pyrolysis of sugarcane bagasse with high density polyethylene using Coats-Redfern methods	194
CHAPTER 5 CONCLUSION AND FUTURE RECOMMENDATIONS		202
5.1	Conclusion	202
5.2	Future recommendations	204
REFERENCES		206
APPENDICES		
LIST OF PUBLICATIONS		

LIST OF TABLES

		Page
Table 2.1	Chemical composition of different types of biomass	16
Table 2.2	Several findings regarding synergetic effects between biomass and plastic in co-pyrolysis.	26
Table 2.3	Comparison of products obtained from co-pyrolysis and catalytic co-pyrolysis of biomass and plastics	48
Table 2.4	Comparison of products obtained from co-pyrolysis and catalytic co-pyrolysis of biomass and plastics	53
Table 2.5	Kinetic models of Coats-Redfern method (Zhao et al., 2018, Magalhães et al., 2017; Vyazovkin et al., 2011; White et al., 2011)	57
Table 2.6	Kinetic of co-pyrolysis and catalytic co-pyrolysis of biomass with plastic by thermogravimetric	60
Table 3.1	List of gases	65
Table 3.2	List of chemicals	66
Table 4.1	Proximate and ultimate analyses of raw materials	85
Table 4.2	Elemental composition and heating values of co-pyrolysis oil (Reaction conditions: Reaction time = 45 min; temperature = 600 °C for SCB/HDPE and 500 °C for SCB/PET, mass of SCB and HDPE mixture = 6 g)	119
Table 4.3	Comparison of product distribution and chemical compositions obtained from co-pyrolysis of SCB/HDPE and SCB/PET	121
Table 4.4	Textural characteristic of the FAU-EAFS and HAP-ZE	126
Table 4.5	Experimental and theoretical yield of hydrocarbons and synergistic effect obtained under different SCB: HDPE ratios over FAU-EAFS catalyst	152
Table 4.6	Experimental and theoretical yield of hydrocarbons and synergistic effect obtained under different SCB: HDPE ratios over HAP-ZE catalyst	152
Table 4.7	Comparison of product distribution and chemical compositions obtained from co-pyrolysis of SCB and HDPE over FAU-EAFS and HAP-ZE catalysts	155

Table 4.8	Elemental composition and heating values of pyrolysis oil obtained from thermal pyrolysis of SCB and catalytic co-pyrolysis of HDPE and SCB over FAU- EAFS and HAP-ZE (Reaction conditions: Reaction time = 45 min; temperature = 500 °C for FAU-EAFS and 600 °C for HAP-ZE, mass of SCB and HDPE mixture = 6 g)	156
Table 4.9	Experimental and theoretical yield of hydrocarbons and synergistic effect obtained under different SCB: PET ratios over FAU-EAFS catalyst	180
Table 4.10	Experimental and theoretical yield of hydrocarbons and synergistic effect obtained under different SCB: PET ratios over HAP-ZE catalyst	180
Table 4.11	Comparison of product distribution and chemical compositions obtained from co-pyrolysis of SCB and PET over FAU-EAFS and HAP-ZE catalysts	182
Table 4.12	Elemental composition and heating values of pyrolysis oil obtained from thermal pyrolysis of SCB and catalytic co-pyrolysis of SCB and PET over FAU-EAFS and HAP-ZE. (Reaction conditions: Reaction time = 45 min; temperature = 500 °C, mass of SCB and PET mixture = 6 g)	183
Table 4.13	Pyrolysis characteristics for the thermal, co-pyrolysis and catalytic co-pyrolysis of sugarcane bagasse and high-density polyethylene	193
Table 4.14	Kinetic parameters from the chemical reaction models of the Coats-Redfern method	197
Table 4.15	Kinetic parameters from the diffusion models of the Coats-Redfern method	198
Table 4.16	Kinetic parameters from the power law models of the Coats-Redfern method	199
Table 4.17	Kinetic parameters from the Avrami-Erofe'ev models of the Coats-Redfern method	200
Table 4.18	Kinetic parameters from the contracting model of the Coats-Redfern method	201

LIST OF FIGURES

		Page
Figure 2.1	Chemical structure of lignocellulosic biomass (a) Cellulose; (b) Hemicellulose; (c) Lignin (Hansen and Plackett, 2008; Shahzadi et al., 2014)	15
Figure 2.2	Breakdown of plastic production by plastic resin type in Malaysia (National Solid Waste Management Department, 2011)	19
Figure 2.3	The schematic diagram of co-pyrolysis of biomass and plastic	22
Figure 2.4	Proposed decomposition pathway of the co-pyrolysis of CE and HDPE	25
Figure 2.5	Reaction mechanism between biomass model compounds and polyethylene at catalyst sites (1) Diels–Alder reaction mechanism; (2) hydrocarbon pool mechanism; (3) hydrogen transfer between polyethylene and lignin (Xue et al., 2016)	36
Figure 3.1	Flow chart of overall experimental work	64
Figure 3.2	Schematic diagram of pyrolysis fixed bed reactor	67
Figure 4.1	(a) Thermogravimetric and (b) derivative thermogravimetric curves of SCB, HDPE, and PET at heating rate of 10 °C/min	87
Figure 4.2	Pyrolysis product yield of individual material at different temperature (a) SCB, (b) HDPE and (c) PET. (Reaction conditions: reaction time = 45 min; mass of each SCB, HDPE and PET = 6 g)	89
Figure 4.3	Effect of reaction temperature on the experimental product yields derived from co-pyrolysis of (a) SCB and HDPE and (b) SCB and PET. (Reaction conditions: reaction time = 45 min; mass of each SCB/HDPE and SCB/PET mixture = 6 g, HDPE:SCB and PET: SCB ratio = 40:60)	91
Figure 4.4	Difference between experimental and theoretical products yield at different reaction temperatures derived from co-pyrolysis of (a) SCB and HDPE and (b) SCB and PET. (Reaction conditions: reaction time: 45 min; mass of each SCB/HDPE and SCB/PET mixture = 6 g, HDPE: SCB and PET: SCB ratio = 40:60)	93

Figure 4.5	Effect of reaction temperature on the chemical composition of pyrolysis oil from co-pyrolysis of (a) SCB and HDPE and (b) SCB and PET. (Reaction conditions: reaction time = 45 min; mass of each SCB/HDPE and SCB/PET mixture = 6 g, HDPE: SCB and PET: SCB ratio = 40:60)	97
Figure 4.6	Difference between experimental and theoretical chemical compositions at different reaction temperatures derived from co-pyrolysis of (a) SCB and HDPE and (b) SCB and PET (Reaction conditions: reaction time = 45 min; mass of each SCB/HDPE and SCB/PET mixture = 6 g, HDPE:SCB and PET:SCB ratio = 40:60)	100
Figure 4.7	Evolution of non-condensable gases from co-pyrolysis of (a) SCB/HDPE and (b) SCB/PET in the temperature range of 200–700 °C. (Reaction conditions: Mass of each SCB/HDPE and SCB/PET mixture = 6 g, SCB: HDPE ratio and SCB:PET ratio = 60:40)	104
Figure 4.8	Effect of biomass-to-plastic ratio on the experimental product yields derived from co-pyrolysis of (a) SCB/HDPE and (b) SCB/PET. (Reaction conditions: reaction time = 45 min; temperature = 600 °C for SCB/HDPE and 500 °C for SCB/PET, mass of each SCB/HDPE and SCB/PET mixture = 6 g)	107
Figure 4.9	Difference between experimental and theoretical products yield at different biomass-to-plastic ratio derived from co-pyrolysis of (a) SCB/HDPE and (b) SCB/PET (Reaction conditions: reaction time: 45 min; temperature: 600 °C for SCB/HDPE and 500 °C for SCB/PET, mass of each SCB/HDPE and SCB/PET mixture = 6 g)	109
Figure 4.10	Effect of biomass-to-plastic ratio on the experimental chemical composition from co-pyrolysis of (a) SCB and HDPE and (b) SCB and PET. (Reaction conditions: reaction time: 45 min; temperature: 600 °C for SCB/HDPE and 500 °C for SCB/PET, mass of each SCB/HDPE and SCB/PET mixture = 6 g)	111
Figure 4.11	Difference between experimental and theoretical chemical compositions at different biomass-to-plastic ratios derived from co-pyrolysis of (a) SCB and HDPE and (b) SCB and PET (Reaction conditions: Reaction time = 45 min; temperature = 600	113

	°C for SCB/HDPE and 500 °C for SCB/PET, mass of each SCB/HDPE and SCB/PET mixture = 6 g)	
Figure 4.12	X-ray diffraction pattern of catalysts (a) FAU-EAFS, (b) HAP-ZE	123
Figure 4.13	Nitrogen adsorption desorption isotherms of (a) FAU-EAFS and (b) HAP-ZE	125
Figure 4.14	SEM images and EDX spectra of (a) Hydroxyapatite (HAP) (b) Faujasite-EAF (FAU-EAFS) and (c) Hydroxyapatite-zeolite (HAP-ZE). Magnification = 10000×	129
Figure 4.15	NH ₃ -TPD plot (a) FAU-EAFS, (b) HAP-ZE	131
Figure 4.16	Effect of reaction temperature on the product fractional yields derived from co-pyrolysis of SCB and HDPE over (a) FAU-EAFS and (b) HAP-ZE catalysts. (Reaction conditions: Reaction time = 45 min; catalyst: feedstock ratio = 1:10, mass of SCB and HDPE mixture = 6 g, SCB: HDPE ratio = 60:40)	133
Figure 4.17	Effect of reaction temperature on chemical composition from co- pyrolysis of SCB and HDPE over (a) FAU-EAFS and (b) HAP-ZE catalysts. (Reaction conditions: Reaction time = 45 min; catalyst: feedstock ratio = 1:10, mass of SCB and HDPE mixture = 6 g, SCB: HDPE ratio = 60:40)	135
Figure 4.18	Evolution of non-condensable gases from co-pyrolysis of SCB and HDPE over (a) FAU-EAFS and (b) HAP-ZE in the temperature range of 200–700 °C. (Reaction conditions: Reaction time = 45 min, catalyst: feedstock ratio = 1:10, mass of SCB and HDPE mixture = 6 g, SCB: HDPE ratio = 60:40)	140
Figure 4.19	Effect of catalyst-to-feedstock ratio on product fractional yield from co-pyrolysis of SCB and HDPE over (a) FAU-EAFS and (b) HAP-ZE catalysts. (Reaction conditions: Reaction time = 45 min; temperature = 500 °C for FAU-EAFS and 600 °C for HAP-ZE, mass of SCB and HDPE mixture = 6 g, SCB: HDPE ratio = 60:40)	142
Figure 4.20	Effect of catalyst-to-feedstock ratio on chemical composition from co-pyrolysis of SCB and HDPE over (a) FAU-EAFS and (b) HAP- ZE catalysts. (Reaction conditions: Reaction time = 45 min; temperature = 500 °C for FAU-EAFS and 600 °C for HAP-ZE, mass of SCB and HDPE mixture = 6 g, SCB: HDPE ratio = 60:40)	144

Figure 4.21	Effect of SCB: HDPE ratio on product fractional yield from co-pyrolysis of SCB and HDPE over (a) FAU-EAFS and (b) HAP-ZE catalysts. (Reaction conditions: Reaction time = 45 min; temperature = 500 °C for FAU-EAFS and 600 °C for HAP-ZE, catalyst: feedstock ratio = 1:6, mass of SCB and HDPE mixture = 6 g)	148
Figure 4.22	Effect of SCB: HDPE ratio on chemical compositions from co-pyrolysis of SCB and HDPE over (a) FAU-EAFS and (b) HAP-ZE catalysts. (Reaction conditions: Reaction time = 45 min; temperature = 500 °C for FAU-EAFS and 600 °C for HAP-ZE, catalyst: feedstock ratio = 1:6, mass of SCB and HDPE mixture = 6 g)	149
Figure 4.23	Effect of reaction temperature on the product fractional yields derived from co-pyrolysis of SCB and PET over (a) FAU-EAFS and (b) HAP-ZE catalysts. (Reaction conditions: Reaction time = 45 min; catalyst: feedstock ratio = 1:10, mass of SCB and PET mixture = 6 g, SCB: PET ratio = 60:40)	158
Figure 4.24	Effect of reaction temperature on the chemical compositions derived from co-pyrolysis of SCB and PET over (a) FAU-EAFS and (b) HAP-ZE catalysts. (Reaction conditions: Reaction time = 45 min; catalyst: feedstock ratio = 1:10, mass of SCB and PET mixture = 6 g, SCB: PET ratio = 60:40)	159
Figure 4.25	Distribution of aromatic compounds from catalytic co-pyrolysis of SCB and PET over FAU-EAFS at various reaction temperature (Reaction conditions: Reaction time = 45 min; catalyst: feedstock ratio = 1:10, mass of SCB and PET mixture = 6 g, SCB: PET ratio = 60:40)	162
Figure 4.26	Evolution of non-condensable gases from co-pyrolysis of SCB and PET over (a) FAU-EAFS and (b) HAP-ZE in the temperature range of 200–600 °C. (Reaction conditions: Reaction time = 45 min, catalyst: feedstock ratio = 1:10, mass of SCB and PET mixture = 6 g, SCB: PET ratio = 60:40)	165
Figure 4.27	Effect of catalyst-to-feedstock ratio on product fractional yield from co-pyrolysis of SCB and PET over (a) FAU-EAFS and (b)	168

- HAP-ZE catalysts. (Reaction conditions: Reaction time = 45 min; temperature = 500 °C, mass of SCB and PET mixture = 6 g, SCB: PET ratio = 60:40)
- Figure 4.28 Effect of catalyst-to-feedstock ratio on chemical compositions from co-pyrolysis of SCB and PET over (a) FAU-EAFS and (b) HAP-ZE catalysts. (Reaction conditions: Reaction time = 45 min; temperature = 500 °C, mass of SCB and PET mixture = 6 g, SCB: PET ratio = 60:40) 169
- Figure 4.29 Distribution of aromatic compounds from catalytic co-pyrolysis of SCB and PET over (a) FAU-EAFS (b) HAP-ZE at various catalyst-to-feedstock ratio. (Reaction conditions: Reaction time = 45 min; temperature: 500 °C, mass of SCB and PET mixture = 6 g, PET: SCB ratio = 40:60) 172
- Figure 4.30 Effect of SCB: PET ratio on product fractional yield from co-pyrolysis of SCB and PET over (a) FAU-EAFS and (b) HAP-ZE catalysts. (Reaction conditions: Reaction time = 45 min; temperature = 500 °C, mass of SCB and PET mixture = 6 g, catalyst: feedstock ratio = 1:10 for FAU-EAFS and 1:8 for HAP-ZE) 174
- Figure 4.31 Effect of SCB: PET ratio on chemical compositions from co-pyrolysis of SCB and PET over (a) FAU-EAFS and (b) HAP-ZE catalysts. (Reaction conditions: Reaction time = 45 min; temperature = 500 °C, catalyst: feedstock ratio = 1:10 for FAU-EAFS and 1:8 for HAP-ZE, mass of SCB and PET mixture = 6 g) 176
- Figure 4.32 Distribution of aromatic compounds from catalytic co-pyrolysis of SCB and PET over (a) FAU-EAFS (b) HAP-ZE at various SCB:PET ratio. (Reaction conditions: Reaction time = 45 min; temperature: 500 °C, catalyst: feedstock ratio = 1:10 for FAU-EAFS and 1:8 for HAP-ZE, mass of SCB and PET mixture = 6 g) 178
- Figure 4.33 Effect of types of plastic on (a) Product distributions (b) Chemical compositions. (Reaction conditions: Reaction time = 45 min, temperature: 500 °C, catalyst: feedstock ratio = 1:6 for HDPE and 1:10 for PET, SCB: HDPE and SCB: PET ratio = 40:60) 184

- Figure 4.34 Effect of co-pyrolysis and catalytic co-pyrolysis of SCB with HDPE and PET over FAU-EAFS and HAP-ZE catalysts on (a) Product distributions, (b) Chemical compositions. (Reaction conditions: Reaction time = 45 min, temperature: 500 °C, mass of each SCB/HDPE and SCB/PET mixture = 6 g, catalyst: feedstock ratio = 1:6 for HDPE and 1:10 for PET, HDPE: SCB and PET: SCB ratio = 60:40) 186
- Figure 4.35 (a) Thermogravimetric and (b) derivative thermogravimetric curve for the thermal, co-pyrolysis and catalytic co-pyrolysis of sugarcane bagasse with high density polyethylene over FAU-EAFS and HAP-ZE at heating rate of 10 °C/min 189

LIST OF PLATES

		Page
Plate 3.1	Image of pyrolysis fixed bed reactor	68

LIST OF SYMBOLS

Symbol	Description	Unit
A	Pre-exponential factor	min ⁻¹
E	Activation energy	kJ/mol
g(α)	Mechanism function	-
α	Conversion of the combustible sample	-
$\cdot\text{OH}$	Hydroxyl radical	-
R	Universal gas constant	J/mol·K
R ²	Correlation coefficient	-
T	Absolute temperature	K
w _o	Initial mass of sample	mg
w _f	Final mass of sample	mg
w	Mass of sample at time t,	mg
ΔW	Weight loss	wt%

LIST OF ABBREVIATIONS

BET	Brunauer-Emmett-Teller
BJH	Barret-Joyner-Halenda
BOFS	Basic oxygen furnace slag
CE	Cellulose
CS	Corn stalk
CDM	Clean Development Mechanism (CDM)
CR	Coats-Redfern
DAEM	Distributed activation energy model
DTG	Derivative thermogravimetric
EAFS	Electric arc furnace slag
EDX	Energy dispersive X-ray
FAU-EAFS	Faujasite-electric arc furnace slag zeolite
FWO	Flynn-Wall-Ozawa
GC-MS	Gas chromatography-mass spectrometry
GC-TCD	Gas chromatography-thermal conductive detector
HAP-ZE	Hydroxyapatite-zeolite
HHVs	High heating values
H/C _{eff}	Hydrogen-to-carbon effective ratio
HDPE	High-density polyethylene
IUPAC	International Union of Pure and Applied Chemistry
KAS	Kissinger-Akahira-Sunose
LDPE	Low-density polyethylene
LLDPE	Linear low-density polyethylene

MSW	Municipal solid waste
m/z	Mass to charge ratio
NH ₃ -TPD	Ammonia temperature-programmed desorption
NIST	National Institute of Standards and Technology
PAHs	Polycyclic aromatic hydrocarbons
PAW	Paulownia wood
PC	Polycarbonate
PE	Polyethylene
PET	Polyethylene terephthalate
PP	Polypropylene
PS	Polystyrene
PST	Peach stones
PSW	Plastic solid waste
PVC	Polyvinylchloride
Py-GC/MS	Pyrolysis-gas chromatography/mass spectrometry
RS	Rice straw
SCB	Sugarcane bagasse
SEM	Scanning electron microscopy
TGA	Thermogravimetric analysis
TG	Thermogravimetric
TG-MS	Thermogravimetric -mass spectrometry
WP	Waste newspaper
WS	Walnut shells
XRD	X-ray diffraction
XRF	X-ray fluorescence

YP

Yellow poplar

**CO-PIROLISIS BERMANGKIN KE ATAS HAMPAS TEBU DAN SISA
PLASTIK MENGGUNAKAN PEMANGKIN BERASASKAN ZEOLIT DAN
HIDROKSIAPATIT UNTUK MENGHASILKAN MINYAK PIROLISIS
BERMUTU TINGGI DI DALAM REAKTOR LAPISAN-TETAP**

ABSTRAK

Kesusutan sumber asli, permintaan petroleum yang besar dan kebimbangan alam sekitar telah mencetus motivasi kajian pada bahan api boleh diperbaharui dari biomas. Kajian ini bertujuan menyelidik co-pirolisis dan co-pirolisis bermangkin ke atas hampas tebu (SCB) dan polietilena berkepadatan tinggi (HDPE) atau polietilena teraftalat (PET) di dalam reaktor lapisan tetap pemanasan perlahan menggunakan pemangkin zeolit (FAU-EAFS) dan hidroksiapatit-zeolit (HAP-ZE) yang disediakan dari arka elektrik sanga relau. Dalam proses co-pirolisis, kesan suhu tindak balas (400-700 °C) dan nisbah biomas kepada plastik (100:0-0:100) ke atas hasil keluaran, komposisi kimia dan juga kesan bersinergi telah dikaji. 63.69 wt% hasil cecair optimum dicapai pada 600 °C dan nisbah SCB kepada HDPE 60:40 di dalam co-pirolisis SCB dan HDPE manakala 60.94 wt% hasil cecair dicapai pada 600 °C dan nisbah SCB kepada PET 40:60. Dalam bahagian co-pirolisis bermangkin, kesan suhu tindak balas (400-700 °C), nisbah pemangkin kepada bahan mentah (1:10-1:2) dan nisbah plastik kepada biomas (0:100-100:0) ke atas hasil keluaran dan komposisi kimia telah dikaji. 68.56 wt% and 71.01 wt% maksimum minyak-pirolisis diperolehi dalam co-pirolisis bermangkin SCB dan HDPE menggunakan pemangkin FAU-EAFS dan HAP-ZE. Co-pirolisis bermangkin SCB dan PET menggunakan pemangkin FAU-EAFS dan HAP-ZE, menghasilkan 42.95 wt% and 45.64 wt%, maksimum minyak-pirolisis. Co-pirolisis

bermangkin SCB dan HDPE menggalakkan pengeluaran hidrokarbon dan alkohol manakala co-pirolisis bermangkin SCB dan PET meningkatkan pengeluaran aromatik dan asid. Berbanding HAP-ZE, FAU-EAFS menunjukkan prestasi yang lebih baik dalam pengeluaran hidrokarbon dan aromatik semasa co-pirolisis bermangkin SCB dan HDPE atau PET kerana keasidan yang kuat dan saiz liang yang lebih besar yang meningkatkan tindak balas peretakan dan penyahoksigen dan kecekapan resapan wap pirolisis ke dalam liang pemangkin. Kelakuan pirolisis haba, co-pirolisis dan co-pirolisis bermangkin bagi SCB dan HDPE telah ditentukan menggunakan analisis termogravimetri manakala parameter kinetik telah dikira menggunakan kaedah Coats-Redfern. Di kawasan kedua di mana uraian selulosa dan hemiselulosa menjadi dominan, kolerasi paling sesuai untuk HDPE diperihalkan oleh mekanisme tindak balas kimia tertib pertama, manakala sampel tindak balas lain dikawal oleh model resapan. Manakala, di kawasan ketiga di mana tindak balas di antara SCB dan HDPE berlaku, kesemua sampel tindak balas mengikut mekanisme tindak balas tertib. Penambahan pemangkin FAU-EAFS dan HAP-ZE menghasilkan tenaga pengaktifan yang lebih rendah di kawasan kedua di dalam co-pirolisis bermangkin SCB dan HDPE.

CATALYTIC CO-PYROLYSIS OF SUGARCANE BAGASSE AND WASTE PLASTICS USING ZEOLITE AND HYDROXYAPATITE BASED CATALYST FOR HIGH QUALITY PYROLYSIS OIL IN A FIXED-BED REACTOR

ABSTRACT

Depletion of natural resources, massive demand for petroleum, and environmental concern have motivated studies on renewable fuel from biomass conversion. This study aims to investigate the co-pyrolysis and catalytic co-pyrolysis of sugarcane bagasse (SCB) with high-density polyethylene (HDPE) or polyethylene terephthalate (PET) in a slow-heating fixed-bed reactor over faujasite type zeolite (FAU-EAFS) and hydroxyapatite-zeolite (HAP-ZE) catalysts prepared from electric arc furnace slag. In co-pyrolysis process, the effects of reaction temperature (400-700 °C) and biomass-to-plastic ratio (100:0-0:100) on the products yields, chemical compositions as well as synergistic effect were investigated. The optimum liquid yield of 63.69 wt% was achieved at 600 °C and 60:40 SCB: HDPE ratio in co-pyrolysis of SCB and HDPE while 60.94 wt% of liquid yield was achieved at 600 °C and 40:60 SCB: PET ratio in co-pyrolysis of SCB and PET. In catalytic co-pyrolysis section, the effects of reaction temperature (400-700 °C), catalyst-to-feedstock ratio (1:10-1:2) and biomass-to-plastic ratio (100:0-0:100) on the product yields and chemical compositions were investigated. The maximum pyrolysis oil yield of 68.56 wt% and 71.01 wt% were obtained under catalytic co-pyrolysis of SCB and HDPE over FAU-EAFS and HAP-ZE, respectively. The catalytic co-pyrolysis of SCB and PET over FAU-EAFS and HAP-ZE, produced maximum pyrolysis oil yield of 42.95 wt% and 45.64 wt%, respectively. The catalytic co-pyrolysis of SCB and HDPE promoted the production of

hydrocarbon and alcohol while the catalytic co-pyrolysis of SCB and PET enhanced the aromatic and acid production. Compared to HAP-ZE, the FAU-EAFS showed better performance in the production of hydrocarbon and aromatic during catalytic co-pyrolysis of SCB with HDPE or PET, due to its strong acidity and larger pore size which enhanced cracking and deoxygenation reactions and diffusion efficiency of pyrolysis vapors into the catalyst pore. Thermal pyrolysis, co-pyrolysis and catalytic co-pyrolysis behaviour of SCB and HDPE were determined using thermogravimetric analysis while the kinetic parameters were calculated via Coats-Redfern method. In the second region, where the decomposition of cellulose and hemicellulose are dominant, the best correlation for HDPE can be described by first order chemical reaction mechanism, whereas the other reaction samples are controlled by diffusion model. Meanwhile, in the third region, where the interaction between SCB and HDPE took place, all of the reactions samples followed the order of reaction mechanisms. An addition of FAU-EAFS and HAP-ZE catalysts resulted in lower activation energy in the second region during co-pyrolysis of SCB and HDPE.

CHAPTER 1

INTRODUCTION

1.1 Global Demand for Alternative Energy Sources

Owing to the increasing global energy demand, the supply of non-renewable fossil fuels is expected to be exhausted in the near future, resulting in a global energy crisis. According to a report by the United States Energy Information Administration, (2013), the diminishing coal and crude oil reserves is expected to be depleted by 2112 and 2042, respectively, while the world energy demand will increase by 56% by 2040. The massive consumption of fossil fuel results in amplified emission of detrimental pollutants (sulfur dioxide, nitrogen oxide and carbon dioxide) that triggers environmental problems such as greenhouse effect, global warming and acid rain (Zhang et al., 2016a; Zhao et al., 2018). To mitigate the energy crisis and control the harmful emission of pollutants, several efforts are currently being carried out to search for sustainable and renewable energy sources for the sake of future generations. The renewable energy sources can lessen the dependence on the fossil fuels and minimize negative environmental impact.

As the world's main sustainable energy source, with approximately 100 billion dry tons of annual production globally, biomass resources have a significant potential as alternative energy resource and for possible conversion to useful chemicals due to its low air pollutant emission, renewability and relative abundance (Fan et al., 2018). According to the, International Energy Agency (2011), biofuel consumption will increase in a sustainable manner, from 2% at present to 27% of the total transport fuel global share, until 2050. Utilization of biomass for energy production can reduce CO₂ build up in the atmosphere and reduce global warming because CO₂ released during combustion of biofuel is captured by growing plants through photosynthesis (Vaibhav

and Thallada, 2018). In Malaysia, 75% of the country's land is covered by agriculture site and tropical forest, making biomass as a suitable sources of renewable energy. Malaysian government is keen to utilize the renewable energy for generating electricity and have set an aim to achieve 10% contribution of renewable energy in the total electricity generation by 2020 (Ozturka et al., 2017). In addition, biomass have been recommended as one of the component of Clean Development Mechanism (CDM) for emission reduction project (Mekhilef et al., 2011).

1.2 Biomass-Derived Bio-Oil

Biomass can be converted into bio-oils or intermediate compounds for the chemical industry through thermochemical processes, such as pyrolysis, gasification and combustion (Guedes et al., 2018). Pyrolysis is a thermal degradation process of organic materials at high temperature in the absence of air/oxygen, resulting in three types of products, namely, bio-oil, carbon-rich solids and volatile gaseous components (Dhyani and Bhaskar, 2018). Pyrolysis is regarded to be a front-running technology for the decomposition of biomass into useful intermediate chemical and energy due to its simple operation, reasonable cost, high efficiency, significant mass and volume reduction, efficient energy recovery and various marketable products compare to other competing technologies (Zolghadr et al., 2019; Guedes et al., 2018; Fan et al., 2018).

The liquid produced from pyrolysis is known as pyrolysis oil or bio-oil; this product is a dark brown organic liquid having potential as fuels for numerous purposes and as feedstock for producing hydrocarbons that could be readily incorporated into existing petroleum refineries or future bio-refineries (Campuzano et al., 2019; Özsın and Pütün, 2018). However, biomass-derived bio-oil presents high acidity, high reactivity, high viscosity, low calorific value and low combustion efficiency compared

with conventional oils; these properties limit the application of biomass-derived bio-oil as a direct fuel (Wang et al., 2018a; Fan et al., 2017). Bio-oil can only be directly applied on the equipment that have low requirements of fuels properties such as boilers and kilns (Jin et al., 2019). In addition, previous studies reported that biomass-derived bio-oil generally contain high water content (15–30 wt.%) and oxygenated compounds (35–60 wt.%) such as acids, sugar, aldehyde, phenols, ketone, and furan obtained from biomass moisture and chemical reactions (Guedes et al., 2018; Chen et al., 2016). These characteristics can engender adverse effects on fuel characteristics, including low caloric value, which deteriorates combustion efficiency, corrosion, and instability (Ahmed et al., 2018; Özsın and Pütün, 2018). Therefore, bio-oil quality or the content of the target chemicals should be improved by expelling oxygen through certain upgrading techniques. Addition of an acidic catalyst can deoxygenate bio-oils and enhance the yield and selectivity of hydrocarbon products by means of catalytic cracking and refineries.

1.3 Catalytic Pyrolysis of Biomass

A variety of methods have been undertaken for high efficiency utilization of biomass to achieve high-quality bio-oils. One of them is catalytic pyrolysis technique that involves heating of biomass in the presence of catalyst (Ly et al., 2018; Minh Loy et al., 2018; Yaman et al., 2018). During catalytic pyrolysis, the biomass undergoes thermal decomposition to produce pyrolysis vapor which is then subjected to a list of deoxygenation reaction such as decarbonylation, decarboxylation and dehydration (Shafaghat et al., 2017) where the oxygen was released as carbon monoxide,

carbon dioxide and water. Microporous zeolite such as ZSM-5 have been regarded as an effective catalyst for the production of the aromatic hydrocarbon in

catalytic pyrolysis because of its unique pore structure that favours the aromatic selectivity as well as its efficient cracking and deoxygenation ability resulted from its strong acidity (Ding et al., 2018a; Fan et al., 2017). Aromatic are the valuable component of bio-oils since they are important precursors in the synthesis of polymer and can be utilized as an additive fuel due to its high octane number (Kim et al., 2017c).

Despite the presence of highly efficient catalyst, catalytic pyrolysis is often severely limited by low bio-oil yields, with low aromatics content, and high yield of coke deposit on the catalyst surface resulting the process to be impractical for commercialization (Johansson et al., 2018; Zheng et al., 2018). Coke is a solid deposit that formed on the external surfaces of catalysts due to the heterogeneous reactions of primary pyrolysis vapors (Li et al., 2013). Coke deposition inside the catalyst pore could poison the active site, alter the catalyst topology and textural characteristics (Kabir and Hameed, 2017) and inhibit the capillary and diffusion flow of biomass-derived pyrolysate resulting in low yield of desired products (Galadima and Muraza, 2015). Lower yield of aromatic hydrocarbons and higher coke formation could be attributed to the oxygen rich and low hydrogen-to-carbon effective ratio of biomass ($H/C_{\text{eff}} = 0-0.3$), which in turn leads to the creation of hydrogen-deficient hydrocarbon pool and reduction of the biomass conversion efficiency (Johansson et al., 2018; Zheng et al., 2018). Hydrogen-poor hydrocarbon pool leads to high degree of polymerization of pyrolysis-derived compounds and the enhanced growth rate of coke precursors (Rezaei et al., 2017).

1.4 Catalytic Co-Pyrolysis

Co-feeding of carbon and hydrogen-rich materials into catalytic pyrolysis of biomass could be an effective approach to attenuate the problem related to coke deposits

on the micropore zeolite catalyst, leading to improved catalytic activity and increased production of desirable chemicals (Zhou et al., 2019; Shafaghat et al., 2018;). Özsın and Pütün (2018) reported that co-feeding hydrogen deficient biomass and its derivatives with hydrogen-rich feedstock is a practical solution to improve the overall H/C_{eff} of feedstock. A feedstock with high H/C_{eff} ratio can serve as hydrogen supplement for biomass conversion and balance the contents of carbon, hydrogen, and oxygen in the feedstock, leading to positive synergistic effect on enhancing bio-oil quality. Synthetic polymers such as waste plastics represents as an ideal co-reactant in catalytic pyrolysis of biomass because it is abundant, cheaper and rich in hydrogen source (e.g., ~14–15 wt.% for polyethylene (PE) and polypropylene (PP)) able to enhance the aromatic yield and lessen the coke formation (Jin et al., 2019; Burra and Gupta, 2018). Furthermore, the fuel produced from pyrolysis of plastics can be regarded as clean and have high calorific value, similar to commercial petroleum fuels due to absence of water content in the fuels. Duan et al. (2017) reported that the bio-oil yield increased from 19.20 wt% to 59.42 wt% while the coke yield decreased about 1% with increasing H/C_{eff} of the feedstock.

Although this upgrading process is effective in enhancing the aromatic hydrocarbon production, the hindering effect in diffusion of plastic molecules and biomass-derived molecules such as levoglucosan into the small pores of microporous zeolites during catalytic co-pyrolysis was identified as a major problem (Chi et al., 2018; Kim et al., 2017c). The microporous zeolite possesses diameter of less than 1 nm which is unfavourable in the catalytic activity of the large reactant molecules. The bulky size of biomass molecules and plastic-derived pyrolyzates formed during the primary stages of pyrolysis are unable to penetrate into the microporous catalytic active sites. The property of co-reactant materials and also the properties of acid catalyst such as

pore size and acid strength play a pivotal role in determining the efficiency of aromatic production (Rezaei et al., 2017). Hong et al. (2017) studied the pore size effect of microporous and mesoporous HZSM-5 towards the production of aromatic hydrocarbon in co-pyrolysis of cellulose and polypropylene. The authors reported that the formation of aromatic hydrocarbon was favoured on mesoporous HZSM-5 synthesized by the desilication of microporous HZSM-5. The presence of larger pore opening facilitate the diffusion of wider range of molecular sizes into the catalyst pore. For this reason, the use of mesoporous catalyst can be an effective solution to enhance the catalytic interaction of the pyrolysis product of the model biomass compounds (cellulose, xylan, and lignin) and plastic at the catalytic site of the zeolite catalyst by hydrogen transfer, Diels–Alder reaction, and hydrocarbon pool mechanism.

Going further in line with the green chemistry principles, the utilization of mesoporous catalyst from the low-cost materials recently gain considerable attention. Steel slag is a by-product material generated by steelmaking industries (Qazizadeh et al., 2018). Two most commonly steel slag produced are electric arc furnace slag (EAFS) and basic oxygen furnace slag (BOFS). Disposal of this material requires large land area and is uneconomical. From the perspectives of waste management and environmental conservation, converting these slags into value-added material is considered as a cleaner approach to circumvent the issues of waste disposal. The primary constituents of the slag are SiO_2 , Al_2O_3 , Fe_2O_3 , CaO , and little amount of transition metal (Nasuha et al., 2016; Kuwahara et al., 2009) which could be suitable to be converted to value added materials such as cheap adsorbent and catalyst to circumvent the waste disposal issues (Okoye et al., 2017; Kuwahara et al., 2010).

1.5 Problem Statement

In Malaysia, about 168 million tonnes of biomass, including timber and oil palm waste, rice husks, coconut trunk fibres, municipal waste and sugar cane waste has been produced annually. In addition, about one million tonnes of non-recycled plastic waste has been produced every year, making Malaysia as the eight worst country for plastic waste. From the perspectives of waste management and environmental conservation, converting biomass and plastic wastes into value-added material is considered as a cleaner approach to circumvent the issues of waste disposal.

Depletion of natural resources, massive demand for petroleum, and environmental concern have motivated studies on renewable fuel. Biomass pyrolysis has emerged as a frontier thermochemical conversion method in waste treatment due to its capacity to convert biomass into valuable bio-oil; this approach is superior to other competing technologies, such as gasification and high-pressure liquefaction in terms of energy recovery and economic advantages. However, biomass-derived bio-oil suffers from high acidity, high reactivity, high viscosity, low calorific value and low combustion efficiency compared with conventional oils; these properties hinder the application of biomass-derived bio-oil as a direct fuel.

Therefore, catalytic pyrolysis of biomass using various type of catalysts has been suggested as a promising approach to produce a high quality bio-oil. Although the catalytic pyrolysis of biomass can produce liquid fuel that is almost equivalent to petroleum-derived fuels, it also has some drawbacks such as generation of large amount of coke, low yield of valuable hydrocarbons and rapid catalyst deactivation that limit its application for practical utilization. Coke formation happens mainly due to the high oxygen content and low hydrogen to carbon effective ratio of biomass ($H/C_{\text{eff}} = 0-0.3$),

which in turn leads to lower hydrogen content of the hydrocarbon pool and reduction in the biomass conversion efficiency.

Co-feeding of hydrogen rich materials such as polyolefins (PE, PP, PS, and PVC) into catalytic pyrolysis of biomass can be an effective method to reduce the coke deposition and enhance the catalytic activity towards the production of desired compounds. Plastic can act as hydrogen donor to the biomass to balance the percentages of oxygen, carbon and hydrogen in the feedstock, leading to a positive synergistic effect on the improvement of the bio-oil quality.

Microporous zeolite has been extensively used in co-pyrolysis of biomass and plastics because of its unique pore structure that favours the aromatic selectivity as well as its efficient cracking and deoxygenation ability resulted from its strong acidity. However, the microporous size of zeolite (<2 nm) prevents the diffusion of large molecules into its internal acid sites. The bulky molecules of biomass and plastic-derived pyrolyzates formed during the primary stages of pyrolysis are unable to penetrate into the internal pores and make contact with the catalytic acid sites because of their diameter is bigger than the pore size of the microporous zeolite. To circumvent the problems related to the diffusion limitations and accessibility of the bulky molecules, mesoporous catalyst with diameter larger than the microporous zeolite could be a practical approach for effective mass transfer of large molecules and reduction of coke deposition.

Electric arc furnace slag (EAFS) is a by-product material generated by steelmaking industries during the process of melting and initial acid refining of liquid steel. An estimated 20-40 kg of this waste is generated for every ton of steel produced and it is estimated about 12 million tons of EAFS are produced in Europe annually.

Most of the study on co-pyrolysis of biomass and plastics use classical industrial synthetic zeolite such as ZSM-5, H-Beta, mordenite and faujasite. EAFS which consists of complex oxides such as SiO_2 and Al_2O_3 could be a suitable precursor for the production of zeolite-based catalyst. Thus, this material could be a more cost-effective and greener alternative to synthetic zeolite.

1.6 Objectives of the Study

The objectives of this study are to:

- i. Determine the optimum reaction temperature and blending ratio as well as synergistic effect in co-pyrolysis of sugarcane bagasse with high-density polyethylene or polyethylene terephthalate for high quality pyrolysis oil production.
- ii. Prepare and characterize mesoporous faujasite-type zeolite (FAU-EAFS) and hydroxyapatite-zeolite (HAP-ZE) derived from electric arc furnace slag (EAFS).
- iii. Evaluate the optimum reaction temperature, catalyst-to-feedstock ratio and plastic-to-sugarcane bagasse ratio in catalytic co-pyrolysis of sugarcane bagasse with high-density polyethylene or polyethylene terephthalate for high quality pyrolysis oil production.
- iv. Determine the kinetic parameters of thermal, co-pyrolysis and catalytic co-pyrolysis of sugarcane bagasse with the best plastic over FAU-EAFS and HAP-ZE using Coats-Redfern method.

1.7 Scope of Study

The present study covers the production of pyrolysis oil from the slow co-pyrolysis and catalytic co-pyrolysis of sugarcane bagasse (SCB) with two different types of plastics: high-density polyethylene (HDPE) and polyethylene terephthalate (PET) in a fixed bed reactor. The reaction parameters such reaction temperature (400–700 °C) and plastic-to-SCB ratio (100 SCB, 20 plastic: 80 SCB, 40 plastic: 60 SCB, 60 plastic: 40 SCB and 100 plastic) were investigated during co-pyrolysis of SCB with HDPE and PET. The product yield, chemical compositions, gas compositions and synergistic effects obtained from various operating conditions were compared to determine the best reaction conditions.

Two mesoporous catalyst were prepared from electric arc furnace slag (EAFS): faujasite-type zeolite (FAU-EAFS) and hydroxyapatite-zeolite (HAP-ZE). The prepared catalysts were characterized by X-ray diffraction (XRD), nitrogen adsorption-desorption, Scanning electron microscopy–energy dispersive X-ray (SEM-EDX), and ammonia temperature programmed desorption (NH₃-TPD).

The catalytic activities of the prepared catalysts were studied in the co-pyrolysis of SCB with HDPE and PET at different reaction temperature (400–700 °C), catalyst-to-feedstock ratio (1:10 –1:2) and SCB-to-plastic ratio (100 SCB, 80 SCB: 20 plastics, 60 SCB: 40 SCB, 40 SCB:60 plastics, and 100 plastic). The product yields, chemical compositions, and gas compositions obtained from various operating conditions were compared to establish the best reaction conditions. The pyrolysis pattern and kinetic parameters of thermal, co-pyrolysis and catalytic co-pyrolysis of SCB with HDPE are determined using thermogravimetric analyzer.

1.8 Thesis Organization

This thesis comprises of five chapters. The summary of each chapter are presented as below:

Chapter one presents the overview on current scenario of global energy demand and the potential of catalytic co-pyrolysis technique to produce sustainable and renewable fuel and chemicals for future generations. In addition, this chapter also highlights the utilization of biomass and plastic for the production of bio-oil and also the use of greener and cost-effective precursor for the zeolite synthesis. The problem statement, research objectives, scope and organization of thesis were also presented.

Chapter two reviews previous and recent studies on co-pyrolysis, catalytic co-pyrolysis and types of acidic catalysts used in catalytic co-pyrolysis of lignocellulosic biomass with various kinds of plastics. The synergistic effect, reaction conditions (temperature, catalyst-to-feedstock ratio, biomass-to-plastic ratio) and kinetic studies of co-pyrolysis and catalytic co-pyrolysis of lignocellulosic biomass with different types of plastics were also reviewed.

Chapter three outlines the materials, chemicals and equipment used in the study. The experimental procedure for feedstock preparation, catalysts synthesis, catalyst characterization, reactor set-up and co-pyrolysis and catalytic co-pyrolysis are described in this chapter.

Chapter four presents the research findings and extensive discussion of the experimental results. This chapter covers characterization of the feedstock and catalysts, co-pyrolysis, catalytic co-pyrolysis of SCB with HDPE and PET over acidic catalyst on the products yield and chemical compositions together with the oil properties. In addition, the thermal decomposition behaviour and kinetic analysis of co-pyrolysis of

SCB with HDPE with and without the catalysts using the thermogravimetric analysis were extensively clarified. Chapter five presents the primary research conclusions and recommendations for future work related to catalytic co-pyrolysis.

CHAPTER 2

LITERATURE REVIEW

2.1 Introduction

This chapter presents an overview of the previous and recent studies on co-pyrolysis and catalytic co-pyrolysis of plastic and biomass. The amounts of biomass and plastic produced in Malaysia and worldwide are reported and the major components of biomass and plastic are described. This chapter also discusses the steps in producing oil from co-pyrolysis, the mechanism of co-pyrolysis of biomass and plastics and the synergistic effect involved as well as the effects of reaction parameters including reaction temperature and blending ratio on product distribution and chemical compositions. The catalytic co-pyrolysis section discusses the possible reaction mechanism involved during catalytic co-pyrolysis, function and type of acidic catalysts as well as the effects of reaction parameters including reaction temperature, catalyst-to-feedstock ratio and blending ratio on the product distribution and chemical compositions. Lastly, the kinetic studies of biomass and plastic mixture decomposition with and without the catalyst by Coats-Redfern method were also reviewed.

2.2 Feedstock for Co-Pyrolysis Process

2.2.1 Lignocellulosic Biomass

Approximately 220 billion tons of dry biomass is produced worldwide per year, making biomass as the world's largest sustainable energy source (Abnisa and Wan Daud, 2014). Biomass is a preferable source of renewable energy as it can be stored and is readily available throughout the year compared to other sources of renewable energy such as solar, hydro, wind and geothermal (Ozturka et al., 2017). Biomass constitutes around 14% of the world energy supply and can be regarded as the sole source of

renewable energy which can be transformed into different types of fuels (liquid, gaseous, and solid) and valuable chemicals (Mamaeva et al., 2016). Various kinds of biomass are an excellent feedstock for co-pyrolysis. The types of biomass can be classified as crops and their by-products, wood and wood wastes, waste from food processing and aquatic plant, municipal solid waste and algae (Guedes et al., 2018). In Malaysia, about 160 million tonnes of biomass, including timber and oil palm waste, rice husks, coconut trunk fibres, municipal waste and sugar cane waste have been produced annually. The National Biofuel Policy, launched in year 2006 promotes and emphasizes the utilization of environmentally friendly, viable and sustainable sources of biomass energy (Ozturka et al., 2017). Moreover, the Malaysian government under the Five Fuel Policy has acknowledged biomass as one of the potential renewable energy sources (Kardooni et al., 2015). Furthermore, the Malaysian government have also implemented the National Biomass Policy 2020, to exploit the biomass for production of value-added products (Salema et al., 2019).

Sugarcane cultivation is a major sector that contributes waste for biomass energy. More than 700,000 tonnes of sugarcane bagasse are produced annually in the vast sugarcane plantation areas in Northern Malaysia (Shafie et al., 2012). This amount accounts for 30% to 40% of the by-products from sugar production, thereby making sugarcane bagasse an abundant waste in Malaysia. Moreover, this material is commonly used as an additive in the construction industries and as a main source of biofuel (David et al., 2018; Henrique et al., 2018). It is a fibrous solid residue obtained by extraction of sucrose-rich juice from stalks, and is a potential feedstock for biofuel production due to its high volatile matter content (nearly 80% (w/w)) (Ghorbannezhad et al., 2018).

2.2.1(a) Components of Lignocellulosic Biomass

Biomass is typically characterized by complex compositions of cellulose (30%–50%), hemicellulose (15%–35%), lignin (10%–20%), and minor amounts of other organics, such as carbonates, nitrates, moisture, and fluid materials. Figure 2.1 shows the structural components of lignocellulosic biomass for pyrolysis process. The typical chemical compositions of cellulose, hemicellulose and lignin in various lignocellulosic biomass according to its sources are listed in Table 2.1.

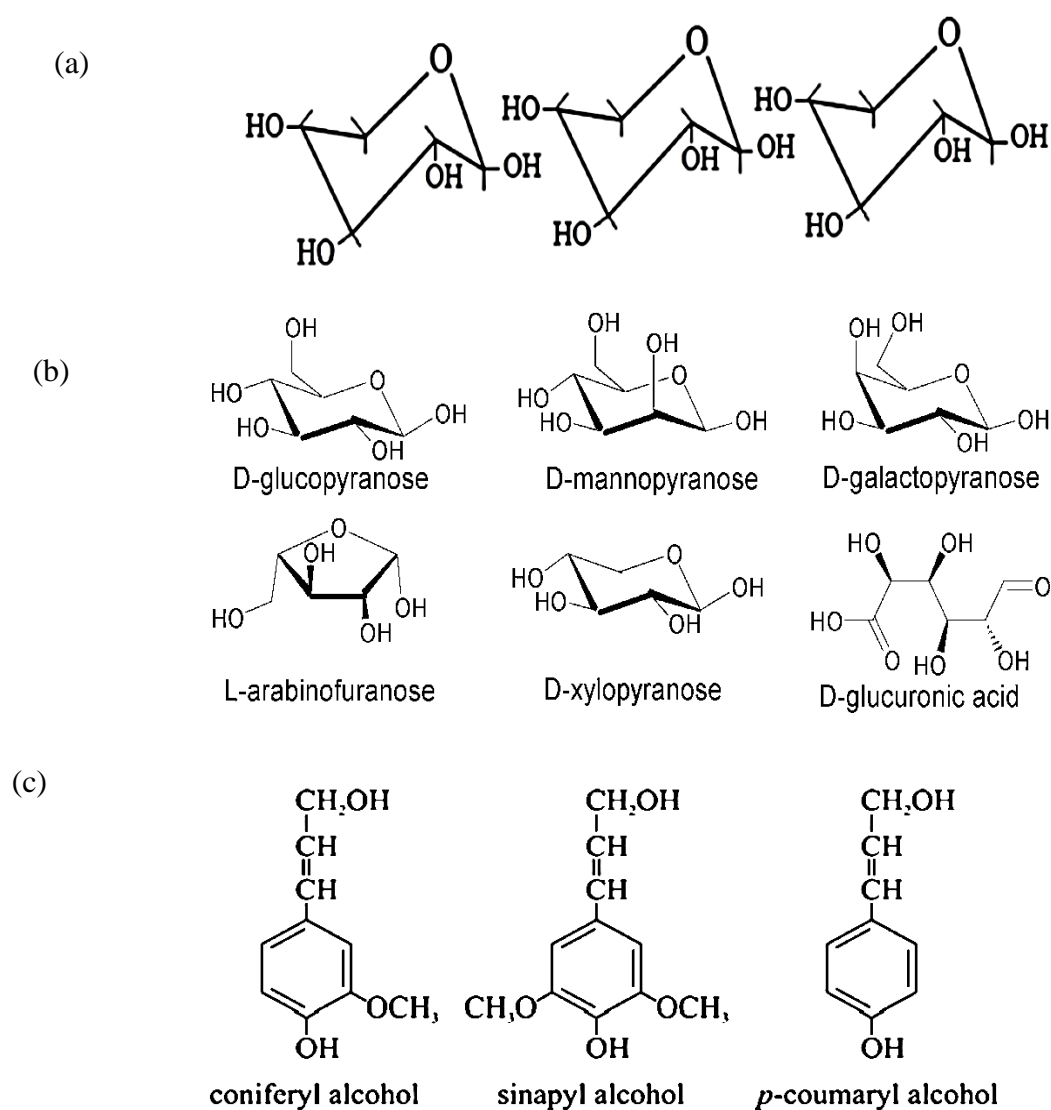


Figure 2.1 Chemical structure of lignocellulosic biomass (a) Cellulose; (b) Hemicellulose; (c) Lignin (Hansen and Plackett, 2008; Shahzadi et al., 2014).

Table 2.1 Chemical composition of different types of biomass

Biomass	Cellulose (%)	Hemicellulose (%)	Lignin (%)	Extractives (%)	Reference
Empty fruit bunch	37.00	35.00	24.00	-	Salema et al., (2019)
Orange bagasse	28.98	31.70	9.52	29.8	Bhattacharjee and Biswas, (2019)
Corn cob	37.63	31.60	20.77	-	Fan et al., (2019)
Palm kernel shell	27.4	22.1	50.5	1.4	Huang et al., (2019)
Sugarcane bagasse	40.75	23.77	26.81	8.67	Ahmed et al., (2018)
Poplar sawdust	54.05	17.96	51.29	-	Wang et al., (2018b)
Wheat straw	32.5	38.3	20.7	8.5	Farooq et al., (2018)
Mallee wood	42.4	23.8	24.7	-	Jiang et al., (2018)
Rice husk	36.23	18.12	24.65	-	Minh Loy et al., (2018)
Jatropha waste	59.20	18.00	22.80	-	Kaewpengkrow et al., (2017)
Durian shell	60.45	13.01	15.45	11.09	Tan et al., (2017)
Pinewood	10.50	48.60	25.30	15.50	Wang and Wang, (2016)
Beech wood	51.30	28.00	19.60	-	Feng et al., (2016)

Cellulose ($[C_6(H_2O)_5]_n$) is a crystalline material and consists of large-molecular-weight polymers derived from a glucose monomer known as pyranose. The crystalline structure of cellulose is made up of three hydroxyl groups in each pyranose ring which can interact with each other forming intra-and intermolecular hydrogen bonds (Vaibhav and Thallada, 2018). Cellulose is more thermally stable compared to hemicellulose because the former lacks branches. Cellulose conversion primarily occurs

between 320 °C and 380 °C with anhydrocellulose and levoglucosan as the primary products (Mamaeva et al., 2016).

Hemicellulose ($[C_5(H_2O)_4]_n$) is an amorphous long-chain polymer with several sugars represented by xylan. Hemicellulose comprised of different monomers include glucose, xylose, mannose, arabinose, galactose and glucuronic acid (Dhyani and Bhaskar, 2018). Decomposition of hemicellulose found at low temperatures ranging from 200 °C to 260 °C yields more volatile components with less tar and char, in contrast to cellulose (Mamaeva et al., 2016). The carbohydrate constituents of the lignocellulosic biomass such as polysaccharide sugar is made of cellulose and hemicellulose.

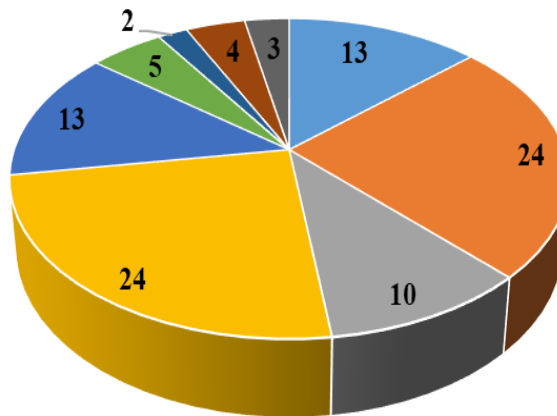
Lignin ($[C_{10}H_{12}O_3]_n$) is the most difficult component for decomposition because of its nature as an aromatic polymer that comprises of sinapyl alcohol, coniferyl alcohol, and *p*-coumaryl alcohol linked by ether bonds or carbon–carbon linkages (Zhang et al., 2015). Among the three constituents of biomass, lignin is the most difficult one to decompose. The decomposition of lignin occurs within a higher temperature range from 200 °C to 500 °C to produce an abundant of oxygenates based on benzene rings, such as phenols (Mamaeva et al., 2016). The decomposition of lignin yields the maximum solid residue (42 wt.%) compared with hemicellulose (32 wt.%) and cellulose (5 wt.%) because of polymerization of lignin fragments via free radical mechanism (Dhyani and Bhaskar, 2018).

2.2.2 Synthetic Polymers

Rapid population growth and expanding urbanization has led to the increase in plastic demand tremendously over the last two decades. Plastic is widely used in various sectors such as households, packaging materials, electronics, automobiles, agriculture,

toys and etc (Jin et al., 2019). The global production of plastics has augmented gradually by 4% every year, from 299 million metric tons in the year 2013 to 355 million metric tons in year 2016 (Plastics Europe, 2016). The continuous rising of plastics demands has led to the growing in plastic solid waste (PSW) accumulation every year. Approximately 30.8% of the total global plastic production comprises of municipal solid waste (MSW) end up in landfill space for disposal, and the remaining percentage is recovered by recycling and energy recovery processes. Polyethylene [PE, low-density (LDPE) and high-density (HDPE)], polypropylene (PP), polystyrene (PS), polyvinylchloride (PVC), and polyethylene terephthalate (PET) are the main plastics found in MSW (Sipra et al., 2018). The highest fraction of total plastic wastes originates from packaging materials, which make up 50%–70% of the total plastic disposal derived from polyolefins (PE, PP, PS, and PVC) (Kunwar et al., 2016).

In Malaysia, approximately 26 million kg of solid waste is generated per day. Plastic is the common solid waste found in MSW, contributing about 7% to 12% by weight and 18% to 30% by volume to the total waste generated by Malaysian residents (Ozturka et al., 2017). Around 2 million tonnes of resins for the plastics industry are produced every year domestically. Figure 2.2 shows the breakdown of plastic production by plastic resin type in Malaysia (National Solid Waste Management Department, 2011). The largest fraction of plastic resin is dominated by HDPE and LDPE (24% each) followed by PET/PETE and PP (13% each).



- Polyethylene terephthalate
- High-density polyethylene
- Polyvinylchloride
- Low density polyethylene
- Polypropylene
- Polystyrene
- Poly(methyl methacrylate)
- Acrylonitrile butadiene styrene
- Polycarbonates

Figure 2.2 Breakdown of plastic production by plastic resin type in Malaysia (National Solid Waste Management Department, 2011).

PP and PE (LDPE and HDPE) are the most used plastics globally. HDPE can be characterised as a high-strength plastic due to its high degree of crystallinity and low branching (Anuar Sharuddin et al., 2016). HDPE has a greater fraction of crystalline regions that make it harder and opaque compared to LDPE (Sogancioglu et al., 2017). HDPE is widely applied as detergent bottles, oil containers, milk bottles and toys, making HDPE the third largest plastic type found in municipal solid waste (MSW) worldwide. PET is an ideal polymer for food packaging industry especially in the production of beverage bottles for mineral water, soft drink and fruit juice because of its inherent characteristic which are lightweight and pressure-resistant containers making it suitable polymer for large-capacity application (Diaz-Silvarrey et al., 2018).

The challenges of plastic waste management and continuous rising of energy demand can be significantly addressed by conversions of these waste plastic to fuels.

Previous study revealed that pyrolysis of plastics alone produces high oil yield, and the derived oil contains almost no oxygen; thus, plastics can be considered as a good feedstock candidate for production of bio-oils. Plastic wastes contain abundance of hydrogen and nearly no oxygen compared with biomass (Kai et al., 2019). The fuel produced from plastics waste is regarded as clean and have high calorific value similar to commercial petroleum fuels due to the absence of water content in the fuels (Sharma et al., 2014). Unlike biofuels, the absence of oxygen in plastic fuels make it non-corrosive and acidic-free (Kunwar et al., 2016). In this regard, the plastic can be a good choice as co-reactant in the pyrolysis of lignocellulosic biomass that can contribute to higher heating value (Tang et al., 2019). Plastics could provide hydrogen to biomass during co-pyrolysis and adjust the contents of carbon, hydrogen, and oxygen in the feedstock, leading to positive synergistic effect on enhancing bio-oil quality (Jin et al., 2019; Johansson et al., 2018; Yuan et al., 2018).

2.3 Co-Pyrolysis Process

Numerous researchers have concentrated on the co-pyrolysis techniques because of their simplicity and capability in operation, which are essential for the production of valuable pyrolysis liquid fuel (Kai et al., 2019; Johansson et al., 2018; Yuan et al., 2018). These techniques do not desire any solvent or catalyst and can be operated without hydrogen pressure. Co-pyrolysis uses two or more diverse materials as feedstock, and the operations are virtually similar to normal pyrolysis techniques. In general, co-pyrolysis occurs in a closed reactor system under moderate operating pressure and temperature with oxygen-free condition. Notably, the liquid yield from co-

pyrolysis is higher than that of normal pyrolysis, between 1.42 and 22 wt.% in general (Abnisa and Wan Daud, 2015). In addition, high calorific value of the liquid product was obtained typically between 26.78-34.79 MJ/kg which is beneficial for engine performance as it has higher thermal efficiencies and power outputs (Chen et al., 2016).

There are three important steps in co-pyrolysis for the production of pyrolysis-oil namely, feedstock preparation, co-pyrolysis, and condensation. In the feedstock preparation steps, the biomass and plastic waste are dried to remove the moisture content, then the feedstock are ground to fine powder and sieved to the desired size (generally less than 2-3 mm) (Zhang et al., 2016a). Smaller particles generally enhance the bio-oil production by suppressing the char formation and secondary cracking of volatile intermediates resulted from enhancement of heat and mass transfer that form uniform temperature within particles during the pyrolysis (Kan et al., 2016).

In the co-pyrolysis stage, inert gas was employed to remove oxygen in the system to create an inert condition before the pyrolysis process take place and to accelerate the movement of vapor produced in reaction zone (pyrolysis zone) to the condenser. Nitrogen gas was commonly used as an inert gas since it is readily available, cheap and inert. Short hot vapor residence time is needed to minimize secondary reactions such as recondensation of char residue, thermal cracking and repolymerization that leads to the reduction in bio-oil yield (Guedes et al., 2018). Higher rate of inert gas that flow into the reactor generally decrease the bio-oil yield, thus an appropriate setting of inert gas flow is essential to obtain the highest yield of bio-oil (Abnisa and Wan Daud, 2014). In the condensation step, the pyrolysis vapor will go through the condensation unit to be transformed from gas to the liquid phase. A high liquid yield was obtained when the pyrolysis vapor undergoes fast cooling process. Vapor

temperature of less than 400 °C is considered detrimental as it causes secondary condensation reaction which lowers the molecular weight of the liquid product. Hence, temperature greater than 400 °C should be fixed along the pipelines from hot zone (pyrolysis zone) to cold zone (condenser) to avoid blockage of the piping system and equipment and also lessen the liquid deposition (Bridgwater et al., 1999). Figure 2.3 represents the schematic diagram of the steps required in a co-pyrolysis system.

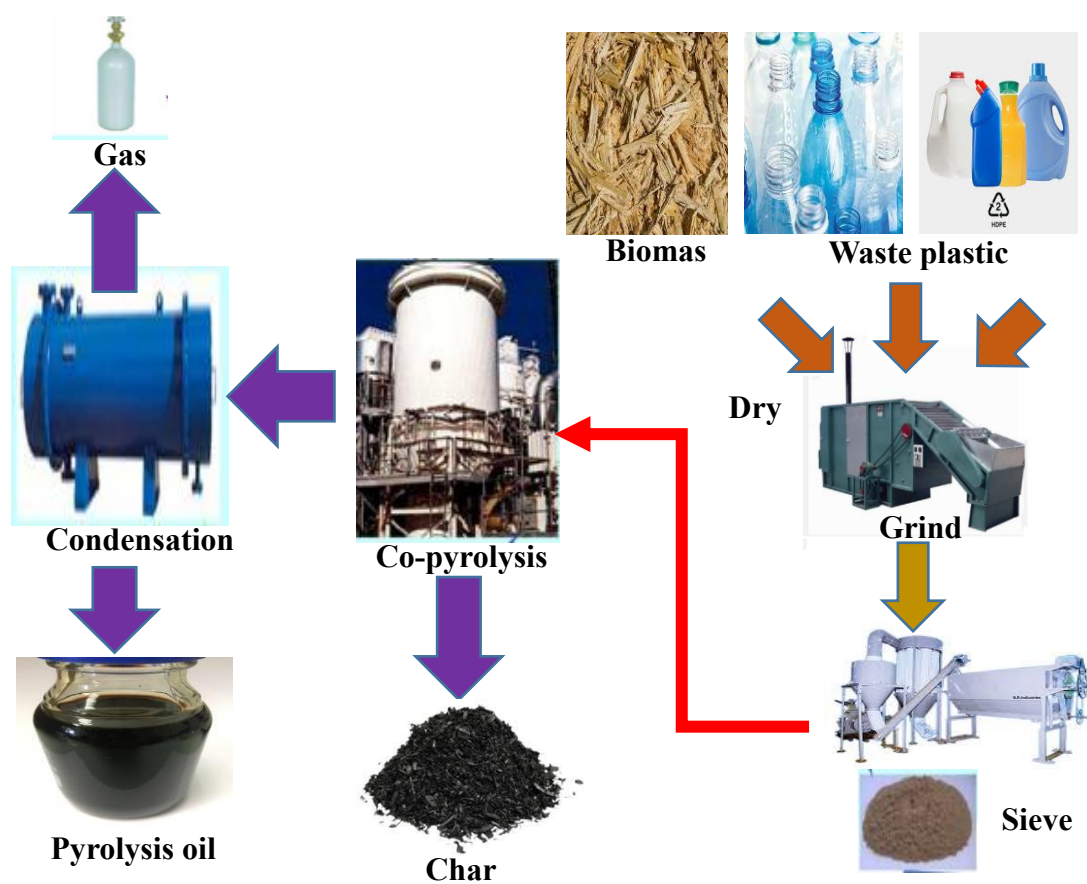


Figure 2.3 The schematic diagram of co-pyrolysis of biomass and plastic

Previous studies have demonstrated that the enhancement in the quality and quantity of the bio-oil was due to the synergistic effect between biomass and plastic (Jin et al., 2019; Lu et al., 2018; Yuan et al., 2018). Synergy can be defined as two or more distinct agents interacting together to produce an effect greater than the values calculated from individual agents (Önal et al., 2014). Several researchers claimed that the synergistic effect between the feedstocks in co-pyrolysis occurs when the

differences between the experimental values and calculated values are positive (Yuan et al., 2018; Chen et al., 2017c; Chen et al., 2016). The positive or negative synergistic effect are determine by the type of contact between the feedstocks (biomass and plastic), feedstocks blending ratio, pyrolysis reaction time and temperature, heating rate, removal or equilibrium of volatiles formed, inclusion of solvents or catalysts and function of hydrogen-donors (Uzoejinwa et al., 2018). Among these factors, the type of contact between the feedstock elements (biomass and plastic), the compositions of the individual elements of the feedstock, and blending ratio are the major factors that inevitably affect the synergistic effect (Sajdak, 2017).

The synergetic effects of co-pyrolysis of plastics and biomass could be attributed to the radical interaction during co-pyrolysis. Biomass and plastic have contrasting thermal decomposition behavior due to the difference in their compositions and structures. Biomass has lower thermal stability compared to plastic which affect their radical degradation mechanism by boosting the decomposition of macromolecules (Chen et al., 2017a). Thermal pyrolysis of biomass occurred by a series of exothermic and endothermic reaction while the thermal pyrolysis of plastic involve radical mechanisms including initiation, propagation and termination (Önal et al., 2014). The decomposition of biomass started at lower temperature than plastic. The free radicals released such as hydroxyl radical with relatively lower thermal stability may promote the depolymerization of plastic (Yuan et al., 2018). Lu et al. (2018) narrated that the interaction between pine wood and polyethylene produced lower char yield (13.8–22.4 wt%) and higher liquid yield (3.7–4.4 wt%) than theoretical yield. On the other hand, the interaction between pine wood and PVC produced more char yield (15.5–27.9 wt%) and lower liquid yield (7.2–14.4 wt%) compared to calculated values. The interaction

between pine wood with polyethylene and polyvinyl chloride reduced the O/C ratio of oil as compared to theoretical values, which enhanced the quality of the oil.

Synergistic effect on the composition and product yield in the co-pyrolysis of almond shell and HDPE were examined by Önal et al. (2014). They highlighted that the co-pyrolysis oil presented higher hydrogen (78% higher) and carbon content (26% higher), lower oxygen content (86% lower) and higher calorific value (38% higher) than oil from the pyrolysis of individual almond shell. The authors also described several possible reaction mechanisms that could occur during the co-pyrolysis of biomass and HDPE including initiation, formation of secondary radicals (depolymerization, generation of monomers, favourable and unfavourable hydrogen transfer reactions, intermolecular hydrogen transfer (formation of paraffin and dienes), and isomerization via vinyl groups) and finally termination by disproportionation or recombination of radicals. Yuan et al. (2018) proposed the possible reaction that can be induced during the decomposition of cellulose (CE) and HDPE, including β -scission, retroaldol condensation, random scission, dehydration, and decarbonylation reactions. The authors also stated that the hydrogen transfer due to scission of HDPE could promote the degradation of an oxygenated compound such as sugar, aldehyde and ketone whereas the CE-derived oxygenated compounds could promote the scission of HDPE (as shown in Figure 2.4). The co-pyrolysis oil was rich in carbon content with less amount of an oxygenated compound. These outcomes imply that the synergistic effect has a positive impact on the enhancement of pyrolysis-oil quality. Chen et al. (2016) reported that the hydrogen supplement by HDPE and cross reaction between HDPE and waste newspaper derived-free radical could hamper the decomposition of functional groups bonded in cellulose structure of waste newspaper resulting in suppressing the generation of gaseous products with low molecular weight and enhancing the